

CONTRACTOR REPORT ARCCB-CR-98009

**STABILITY OF ARRAYS OF  
MULTIPLE-EDGE CRACKS**

**ANTHONY P. PARKER**

**ROYAL MILITARY COLLEGE OF SCIENCE  
CRANFIELD UNIVERSITY, SWINDON, SN6 8LA, UK**

**JUNE 1998**



**US ARMY ARMAMENT RESEARCH,  
DEVELOPMENT AND ENGINEERING CENTER  
CLOSE COMBAT ARMAMENTS CENTER  
BENÉT LABORATORIES  
WATERVLIET, N.Y. 12189-4050**



**APPROVED FOR PUBLIC RELEASE; DISTRIBUTION UNLIMITED**

**19980707 223**

### **DISCLAIMER**

The findings in this report are not to be construed as an official Department of the Army position unless so designated by other authorized documents.

The use of trade name(s) and/or manufacturer(s) does not constitute an official indorsement or approval.

### **DESTRUCTION NOTICE**

For classified documents, follow the procedures in DoD S200.22-M, Industrial Security Manual, Section II-19 or DoD S200.1-R, Information Security Program Regulation, Chapter IX.

For unclassified, limited documents, destroy by any method that will prevent disclosure of contents or reconstruction of the document.

For unclassified, unlimited documents, destroy when the report is no longer needed. Do not return it to the originator.

REPORT DOCUMENTATION PAGE			Form Approved OMB No. 0704-0188	
Public reporting burden for this collection of information is estimated to average 1 hour per response, including the time for reviewing instructions, searching existing data sources, gathering and maintaining the data needed, and completing and reviewing the collection of information. Send comments regarding this burden estimate or any other aspect of this collection of information, including suggestions for reducing this burden, to Washington Headquarters Services, Directorate for Information Operations and Reports, 1215 Jefferson Davis Highway, Suite 1204, Arlington, VA 22202-4302, and to the Office of Management and Budget, Paperwork Reduction Project (0704-0188), Washington, DC 20503.				
1. AGENCY USE ONLY (Leave blank)		2. REPORT DATE June 1998		3. REPORT TYPE AND DATES COVERED Final
4. TITLE AND SUBTITLE  STABILITY OF ARRAYS OF MULTIPLE-EDGE CRACKS			5. FUNDING NUMBERS  Contract No. 8471-AN-06 (70-1S)	
6. AUTHOR(S) Anthony P. Parker				
7. PERFORMING ORGANIZATION NAME(S) AND ADDRESS(ES)  Royal Military College of Science Cranfield University Swindon, SN6 8LA, UK			8. PERFORMING ORGANIZATION REPORT NUMBER  ARCCB-CR-98009	
9. SPONSORING / MONITORING AGENCY NAME(S) AND ADDRESS(ES)  U.S. Army ARDEC Benet Laboratories, AMSTA-AR-CCB-O Watervliet, NY 12189-4050			10. SPONSORING / MONITORING AGENCY REPORT NUMBER	
11. SUPPLEMENTARY NOTES John H. Underwood - Benet Laboratories Project Engineer. Submitted for publication in <i>Engineering Fracture Mechanics</i> .				
12a. DISTRIBUTION / AVAILABILITY STATEMENT  Approved for public release; distribution unlimited.			12b. DISTRIBUTION CODE	
13. ABSTRACT (Maximum 200 words)  The creation and subsequent shedding of arrays of edge cracks is a natural phenomenon which occurs in heat-checked gun tubes, rapidly cooled pressure vessels, and rock, dried-out mud flats, paint, and concrete and in ceramic coatings and permafrost. The phenomenon covers five orders of magnitude in crack spacing. A simple model is developed which indicates that the shedding behaviour is governed by energy release from individual cracks rather than global energy changes. The model predicts that all cracks will deepen until a crack-spacing/crack-depth ratio (2h/a) of 3.0 is achieved, at which stage crack-shedding will commence. Two out of every three cracks will be shed, leading to a new (higher) crack-spacing/crack-depth ratio at which stage growth of all currently active cracks will be dominant.  An approach based upon rapid, approximate methods for determining stress intensity provides good indications of behaviour provided near-surface stress gradients are not excessive. In cases where stress gradients are high, it is shown that it is necessary to employ numerical techniques in calculating stress intensity. Two specific examples are presented, the first at very small scale (heat-check cracking, typical crack spacing 1mm) and the second very large scale (permafrost cracking, typical crack spacing 20m). The predicted ratios for the proportion of cracks shed and for crack-spacing/crack-depth are in agreement with experimental evidence for gun tubes, concrete, and permafrost. The ratios also appear to match experimental observations of 'island delamination' in ceramic coatings and paint films.				
14. SUBJECT TERMS Crack Arrays, Edge Cracks, Crack Shedding, Crack Growth, Fracture, Fracture Mechanics, Residual Stress, Stress Intensity Factor, Permafrost, Mud Flats, Gun Tubes, Concrete			15. NUMBER OF PAGES 20	
			16. PRICE CODE	
17. SECURITY CLASSIFICATION OF REPORT UNCLASSIFIED	18. SECURITY CLASSIFICATION OF THIS PAGE UNCLASSIFIED	19. SECURITY CLASSIFICATION OF ABSTRACT UNCLASSIFIED	20. LIMITATION OF ABSTRACT  UL	

## TABLE OF CONTENTS

	<u>Page</u>
INTRODUCTION .....	1
EXAMPLE AT SMALL SCALE: HEAT CHECKING OF STEEL .....	4
EXAMPLE AT LARGE SCALE: CRACKING OF ARCTIC PERMAFROST .....	5
EXPERIMENTAL EVIDENCE .....	6
CONCLUSIONS .....	7
ACKNOWLEDGEMENT .....	7
REFERENCES .....	7

## LIST OF ILLUSTRATIONS

1.	Surface Topographies .....	10
2.	Edge Cracks and Associated Stress Intensity Factors .....	11
3.	(a) Array of Equal-Length Edge Cracks	
	(b) Situation After First Shedding of 2/3 of Cracks	
	(c) Situation After Second Shedding of 2/3 of Cracks .....	12
4.	Variation of Normalized Stress Intensity (Triangles) and of Per Tip (Squares) and Total Energy Release Rate (Diamonds) as a Function of $h/a$ ..	13
5.	Variation of Stress Intensity with $h/a$ .....	14
6.	(a) Stress Profiles	
	(b) Stress Intensity (Constant Stress)	
	(c) Stress Intensity (Linearly Decreasing Stress) .....	15
7.	Comparison of Approximations with Actual $K$ Values .....	16
8.	Stress Distribution and Associated Approximate Stress Intensity Factors for Typical Arctic Permafrost Scenario in Early February .....	17
9.	Stress Distribution and Associated Accurate Stress Intensity Factors for Typical Arctic Permafrost Scenario in Early February .....	18
10.	Micrograph of Edge-Cracking in a Gun tube .....	19

## INTRODUCTION

There are at least three examples of multiple-crack patterns which exhibit some degree of stability. The first, which exhibits an extremely high degree of stability, concerns collinear periodic arrays of cracks emanating from a pre-existing array of collinear, equally spaced rivet holes. Because of the principal driving force (the force exerted by the rivet itself) and the known, analytic, value of stress intensity for such configurations there is an inexorable, self-correcting, drive to create multiple, equal-length cracks in such a configuration. Since the force exerted by the rivet is automatically adjusted (via a change in local compliance) and because the crack tip nearest any rivet has a higher stress intensity than the more distant tip [1] a symmetric, equal-length array is ensured. The second example, which exhibits somewhat less stability, concerns arrays of radial, periodic cracks emanating from a circular boundary with an applied displacement boundary condition, for example cracks in glass after the passage of a bullet, cracks in ice following a pointed indentation and cracks in dried-out tree stumps.

A third example, which exhibits moderate stability and is considered herein, concerns multiple-edge cracks emanating from a free surface. Multiple cracking from the free surface of an (effectively) semi-infinite body due to tensile stresses in the layer at (or near) the free surface is a natural phenomenon. The surface topography of the cracking of ice-wedge polygons in Arctic permafrost [2], of mud flats in Death Valley, Figure 1(a), and of craze-cracks (heat-checking) at the bore of a gun tube, Figure 1(b), [3] are all strikingly similar, yet they span five orders of magnitude in scale, with the maximum plate dimensions for ice and mud being, respectively, 22 metres and 0.25 metres and with the minimum plate size for craze-cracking being 0.2mm [3].

Consider a system of multiple, equal-length edge cracks of depth  $a$  and spacing  $2h$ . This geometry, together with some relevant stress intensity factor values [4], is presented in Figure 2. Lachenbruch, in his lengthy treatise [2], has shown that linear elastic fracture mechanics can be applied to edge-cracking in ice; he also presented fracture toughness values for such cracking. However Lachenbruch did not explicitly consider an array of edge cracks; instead he calculated contours of elastic stress-relief at the surface resulting from the introduction of a single crack of depth  $a$  into a pre-existing tensile stress system consisting of constant tensile stress over some or all of the prospective crack surface, with zero stress over the remainder. He concludes that the surface stresses resume 95% of their pre-crack level at a distance from the crack equal to 9 x crack spacing (i.e.  $h/a = 4.5$ ). Crucially Lachenbruch also notes that a typical observed  $h/a$  ratio for permafrost cracking is 1.5.

Bazant and co-workers have produced several papers [5 -9] in which are analyzed the sudden cooling of a rock surface and the associated cracking which this produces. Bazant's analysis is based upon an LEFM study of the energy of individual cracks and of all cracks. Bazant argues that crack-shedding will occur as a proportion of the numerous initial equal-length cracks move ahead faster in order that the system may maximise energy release. Crucially Bazant assumes that every other crack is shed (Shedding ratio,  $S = 1/2$ ) and calculates the crack depth at which shedding occurs as a

function of the driving (residual tensile stress) profile and concludes that shedding begins at  $h/a$  ratios which depend upon the local residual tensile stress and are generally in the range  $0.166 \leq h/a \leq 0.666$ . Unfortunately no experimental evidence is presented in support of these predictions.

Both Lachenbruch (ice) and Bazant (rock) assume that the progression of the crack is via a series of fast fracture events when crack tip stress intensity,  $K$ , reaches the Fracture Toughness,  $K_{IC}$ , of the material. However in the case of a gun tube it is known that the history of crack growth may encompass some or all of: Fast Fracture; Environmental Crack Growth; Fatigue Crack Growth. Furthermore there is no longer a single driving mechanism since global residual stresses may be present in the tube from the outset (as a result of the autofrettage process) and others are induced by thermal and/or phase change effects near the bore during firing of the first few rounds. Finally the cyclic pressurization of the tube will subsequently serve to drive cracks by fatigue crack growth.

Detailed work relating to the gun tube problem will be reported elsewhere [10]. However it is important to emphasize that all of the above modes of multiple-crack extension are  $K$  driven, so that any  $K$ -based crack-shedding model is likely to be applicable across modes of crack extension, and in the transition between modes, when these occur consecutively within a structure as in the case of a gun tube.

Figure 3 illustrates the development of crack-shedding in the case where two out of every three cracks are shed, i.e. the shedding factor  $S$  is  $2/3$ . Obviously the stress intensity factor and associated energy changes in this case will differ from Bazant's assumption of  $S=1/2$ . It may therefore be useful to take a simplistic approach which permits the study of  $S$  over a wide range. Re-plotting the results presented in Figure 2 on a logarithmic scale as a direct function of  $h/a$  we obtain the  $K$  variation represented in Figure 4 by triangles.

Note that the variation in  $K$ , although normalized by  $\sigma\sqrt{h}$  does properly represent the relative variation of real  $K$  provided  $h$  is held constant and  $a$  is permitted to vary. Figure 4 also shows the proportionate variation of per tip energy release rate, obtained by squaring  $K$ . Finally the proportionate variation of total energy release rate for all tips, obtained by summing over all cracks for a given  $h/a$ , is also plotted. From this presentation we conclude:

- a. If maximum total energy release rate drives crack-shedding, either this is maximized by *reducing*  $h/a$ , an effect which is not observed, or cracks do not shed, which also contravenes experimental observation. Total energy release rate is therefore rejected as an explanation for crack-shedding.
- b. That the energy release rate for an individual crack is maximized, with fixed  $h$ , by increasing  $h/a$  to 1.5; any further increase in  $a$  will actually reduce energy release rate slightly.

Having rejected total energy now consider the option of crack-shedding in order to maximize the energy release rate of an individual crack; since energy release is directly proportional to  $K^2$ , all subsequent argument is based directly upon  $K$  variation. Figure 5 shows proportionate variations in real  $K$  values; this is because the normalizing term,  $K_0 = \sigma\sqrt{h_i}$ , where  $h_i$  is the initial crack spacing. In the case of fixed  $h$  and varying  $a$ , movement from right to left along the lower(continuous) curve represents crack deepening, which occurs incrementally.

Starting with  $h$  fixed, from a typical observed initial value of  $h/a > 4$ ,  $K$  increases with increasing  $a$  until at  $h/a = 1.5$  (i.e.  $2h/a = 3$ ).  $K$  cannot increase further by increasing  $a$  and the only option is to begin to 'shed' a proportion of the cracks. If it were possible to achieve such shedding by a 'healing' process in which a proportion of the cracks have their surfaces brought back into contact, the change in  $K$  would be that illustrated for fixed  $a$  and varying  $h$  in the upper (dotted) curve. The  $h/a = 1.5$  point on the lower curve has its  $h/a$  value increased by a factor of  $1/(1 - S)$  in moving to  $h/a = 1.5/(1 - S)$  if a proportion  $S$  of the cracks were 'healed' with its associated stress intensity from the lower curve increased by a factor of  $\sqrt{1/(1 - S)}$ . 'Healing' is clearly physically unreal but will serve as an indicator and a bound for the shedding process. In such a process we note that  $K$  would increase dramatically. Since only integer numbers of cracks can be shed, and periodic symmetry must be maintained, a crack starting from  $h/a = 1.5$  could move to  $h/a = 3, 4.5, 6, 7.5, \dots$  etc.. These integer options are indicated by open boxes along the dotted curve. Of these options  $h/a = 3$  will serve to achieve a 38% increase in  $K$ , 4.5 gives 46%, 6.0 gives 47% etc.. However, the  $h/a = 4.5$  option also permits a transition to significant amounts of energy release during subsequent crack deepening and is a prime candidate.

Returning to the physical unreality of 'healing', in order to identify a more physically acceptable bound, assume that in the natural progression, as a result of variations in material properties, grain size etc., a proportion,  $S$ , of the cracks do indeed move more slowly than their neighbours such that the deeper cracks are 1.5 times the depth of the shorter. A heuristic appeal to St Venant and a knowledge of the behaviour of arrays of deep cracks, indicates that the influence of the shorter cracks will now be much less significant. (This matter is discussed in more detail in an upcoming section). The  $K$  variation resulting from this situation is shown as the upper discrete points (filled boxes) in Figure 5; any integer point on the 'healing' curve has its  $h/a$  ratio decreased by  $1/3$  and its  $K$  value increased in proportion to the ratio of the  $K$  values relating to these two  $h/a$  values extracted from the lower curve in moving to these discrete points. The overall argument relating to the relative changes in  $K$  is, however, unchanged.

The clear implication of the form of presentation in Figure 5 is that, to increase  $K$ , cracks may all deepen until  $h/a \cong 1.5$  followed by the shedding of a proportion equal to  $2/3$  by deepening of the remainder to create a new effective  $h/a \cong 4.5$  whereupon the option of increasing  $K$  by further shedding is removed and the cycle repeats itself by deepening of the currently active (deeper) cracks. The range of  $h/a$  over which deepening and shedding progresses is therefore strikingly limited to  $1.5 \leq h/a \leq 4.5$

which is *precisely the region within which the short and deep crack limiting solutions do not apply.*

## EXAMPLE AT SMALL SCALE : HEAT CHECKING OF STEEL

A more intuitive presentation which permits some understanding of the effect of stress gradients, is shown in Figure 6. Typical stresses and crack depths associated with the craze-cracking of the surface of a steel gun tube are assumed. Two prospective stress profiles are shown in Figure 6(a). They consist of a constant pre-existing stress field of 800MPa into which cracks will be introduced and of a linearly decreasing field with a maximum value of 800MPa. Stress fields which increase with depth are not observed in practice.

Accepted approximations to stress intensity are based upon direct stress normal to the prospective crack line at the prospective crack tip location, designated  $\sigma^*$  [11, 12]. For a single-edge crack the variation of  $K$  with depth, based upon  $K = 1.12\sigma * \sqrt{\pi a}$ , [11], is shown as a heavy curved line; Figure 6(b) relates to constant stress and 6(c) to linearly reducing stress.

However these profiles are modified in the case of multiple cracking, the maximum value at small  $h/a$  being effectively 'capped' at  $K = \sigma * \sqrt{h}$  [12]. Figures 6(b) and 6(c) illustrate such capping for three typical  $h$  values ( $h = 0.2\text{mm}$ ,  $0.6\text{mm}$  and  $1.8\text{mm}$  respectively).

Consider first the case of constant stress, Figure 6(b). An array of very short edge cracks with  $h = 0.2\text{mm}$  may deepen, by increasing  $a$ , until reaching a depth of approximately  $0.13\text{mm}$  at which point  $K$  cannot increase further without the shedding of a proportion of cracks in order to move asymptotically towards the heavy (single-edge crack) line. Furthermore such a shift cannot take place by moving vertically from a point on the 'capped' horizontal line, since this is equivalent to the 'healing' of a proportion of the cracks. A schematic of such a shift is illustrated as is the case of subsequent capping at  $0.4\text{mm}$  and further shedding. In the case of constant stress these shedding processes may be expected to continue to repeat.

Any shift may be expected to be gradual and towards a point which is outside the 'interaction range', a term coined in [13] to indicate the difference in depth between a longer and shorter crack within a periodic array of such cracks at which the influence of the shorter crack upon the stress intensity of the longer crack becomes insignificant. The determination of interaction range for cracks of the periodicity and within the  $h/a$  range of interest here is not addressed in [13]. A discussion relating to the asymptotic bounds on 'interaction range' is in preparation [14]. In order to proceed with the present analysis it is assumed pragmatically that 'interaction range' is approximately equal to  $h$ .



In the more physically realistic case of linearly decreasing stress, Figure 6(c), the heavy curved (single-edge crack) line represents an upper bound on possible  $K$  values; this curve and all 'capping' lines go through a single point at  $a = 0.67\text{mm}$  (the point of zero stress). The argument relating to the point at which shedding begins is similar to the case of constant stress, but the availability of a full 'interaction range' in which shedding can occur is now far more limited. There is the possibility of one, or at most two, shedding cycles before crack arrest occurs. Of crucial importance is the threshold value of  $K$  at which crack extension ceases. This may relate to a threshold for fast fracture, fatigue crack growth or environmental crack growth. The latter is of prime concern in the early stages of crack formation in a gun tube and a typical value of  $13\text{MPa}\sqrt{\text{m}}$  (typical of hydrogen cracking in gun steel) is assumed. With this additional bound on crack extension, designated KSCC, a maximum of one shedding cycle may occur with arrest at approximately 0.2mm crack depth.

Note that the use of  $\sigma^*$  provides an acceptable approximation to  $K$  provided the stress gradient is not excessive. This point is illustrated in Figure 7 which repeats the approximate bounds, based upon  $\sigma^*$  from Figure 6(c) and also shows calculations of actual  $K$  profiles. The method used to obtain  $K$  is of extremely high accuracy (errors  $< 0.5\%$ ) and involves the modified mapping collocation technique, [15] packaged as weight function data [16]. With this correction to  $K$  profiles the predicted crack depth at arrest is increased slightly to approximately 0.22mm. In a further paper [10] a more detailed analysis of the gun tube problem is undertaken and more accurate numerical methods are indeed found to be necessary in order to adequately characterise  $K$  in such high stress gradients.

## EXAMPLE AT LARGE SCALE : CRACKING OF ARCTIC PERMAFROST

To illustrate the application of this approach at large scale consider the problem of cracking of Arctic permafrost, discussed at length by Lachenbruch [2]; such cracking is reported to be most dramatic in early February each year. The heavy curve in Figure 8 shows the variation of stress as a function of depth on 1 February 1954. This curve is based upon temperature variation with depth taking account of the self-weight of the permafrost and is extracted directly from Figure 9 in [2]. Figure 8 also shows the value of stress intensity for a single-edge crack and for arrays of cracks based upon  $\sigma^*$  and the accepted approximations used in the previous section. Three examples of semi-crack spacing,  $h$ , are shown, namely  $h = 1, 3$  and  $9\text{ m}$ .

Interpreting Figure 8 in analogous fashion to the previous section multiple cracks with  $a < 0.5\text{m}$  and with  $h = 1\text{m}$  show rapidly increasing  $K$  until 'capped' by the array effect at around 0.5m depth.  $K$  may then only increase further by 'shedding' and moving asymptotically to the  $h = 3\text{m}$  curve.

From the  $h = 3\text{m}$  curve cracks may shed to  $h = 9\text{m}$  since there is available a full 'interaction range' (i.e. 3m) for shedding. However, once established at  $h = 9\text{m}$  a full

'interaction range' (now 9m) is not available for shedding and the cracks are effectively 'trapped' at their current  $h$  value of 9m and will be forced to arrest when  $K$  drops to  $K_{IC}$  (approximately  $0.3 \text{ MPam}^{1/2}$  for ice) giving a crack depth of around 5m and crack spacing ( $2h$ ), or plate size, of 18m. These figures are each in reasonable agreement with the average of observations reported in [2].

In a similar fashion to the preceding section more accurate (MMC)  $K$  calculations were performed. MMC results analogous to the approximate results in Figure 8 are shown in Figure 9. The way in which crack-shedding and extension occurs is clearly similar to that argued for the approximate case, but with crack depths extending somewhat deeper to 6.5m. This figure is in excellent agreement with the average of observations reported in [2].

## EXPERIMENTAL EVIDENCE

Figure 10 shows the edge-cracking which developed at the bore of a large caliber gun tube [3] and progressed via heat-checking and fatigue processes, both  $K$ -driven. The deepest of the cracks is approximately 0.5mm in a wall of 50mm total thickness. It appears that the initial cracking exhibited an  $h/a$  ratio greater than 4. The inferred crack history appears to follow that illustrated schematically in Figure 3. Crack growth clearly begins at  $h/a$  of approximately 4.5 and continues until  $h/a$  is approximately 1.5, whereupon shedding occurs and the process is repeated twice more. The ratio  $S$  appears to be  $2/3$  throughout.

If such shedding does occur then a histogram of crack depth distributions should appear bimodal. Gough and Morrison [3] have counted numbers and depths of cracks, and at least two of the associated histograms do appear bimodal.

In analyzing the surface topography of cracked concrete Bazant and Cedolin [9] note that an energy-based analysis predicts that cracking will progress by the associated surface effect of the creation and shedding of hexagonal patterns; at each shedding event, hexagons whose 'diameter' is three times larger are created. Note that such a surface effect is equivalent to the value of  $h$  in our two-dimensional analysis increasing threefold (i.e.  $S=2/3$ ), as predicted from the simple model presented herein. Reference [9] also reports that such hexagonal cracking is, indeed, observed in concrete. It is therefore somewhat surprising that throughout References [5 - 9] a value of  $S=1/2$  is assumed.

On a much larger scale, Lachenbruch [2] reports permafrost ice crack  $h/a$  ratios of 1.5 wherein  $h$  may be as large as 22 metres.

Finally, recent experimental observations on 'island-delamination' in brittle coatings of varying depth [17] produce convincing evidence of a consistent  $2h/a$  ratio of 3:1 for ceramic films of up to 0.4 mm depth and paint films of up to 0.1mm depth. In the terms

of [17] the distance  $2h$  used herein is equivalent to the island diameter and  $a$  is equivalent to the film thickness (i.e. maximum depth of cracks).

## CONCLUSIONS

The creation and subsequent shedding of arrays of edge cracks is a natural phenomenon ranging from heat-checking of gun tubes to cracking of permafrost covering five orders of magnitude in crack spacing. The shedding behaviour appears to be governed by energy release from individual cracks rather than global energy changes.

The model developed herein predicts that all cracks will deepen until a crack-spacing/crack-depth ratio ( $2h/a$ ) of 3.0 is achieved, at which stage crack-shedding will commence; two out of every three cracks will be shed, leading to a larger crack-spacing/crack-depth ratio at which stage growth of all currently active cracks will be dominant.

An approach based upon rapid, approximate methods for determining stress intensity provides good indications of behaviour provided near-surface stress gradients are not excessive. In cases where stress gradients are high it is shown that it is necessary to employ numerical techniques in calculating stress intensity.

Two specific examples are presented, the first at very small scale (heat-check cracking, typical crack spacing 1mm) and the second very large scale (permafrost cracking, typical crack spacing 20m).

The predicted ratios for the proportion of cracks shed and for crack-spacing/crack-depth are in agreement with experimental evidence for gun tubes, concrete and permafrost. The ratios also appear to match experimental observations of 'island delamination' in ceramic coatings and paint films.

## ACKNOWLEDGEMENT

Much of this work was undertaken during an attachment to the US Army Armament Research, Development and Engineering Center, Watervliet, NY. The attachment was arranged via the European Research Office of the US Army Research, Development and Standardization Group (UK).

## REFERENCES

- [1] Parker, A. P., The Mechanics of Fracture and Fatigue - An Introduction, E & F N Spon, London, 1981.

- [2] Lachenbruch, A. H., Mechanics of Thermal Contraction Cracks and Ice-Wedge Polygons in Permafrost, Geological Society of America Special Paper, 69 pages, Waverly Press, Baltimore, 1962.
- [3] Gough, J. P. and Morrison, J., Craze Cracking in 105mm Artillery and Tank Gun Barrels, Canadian Defence Research Establishment Pacific, Technical Memorandum 84-9, November 1984.
- [4] Tada, H., Paris, P. C., Irwin, G., The Stress Analysis of Cracks Handbook, Second Edition, Paris Productions Incorporated & Del Research Corp, St Louis, 1985.
- [5] Bazant, Z. P. and Ohtsubo, H., Stability Conditions for Propagation of a System of Cracks in a Brittle Solid, Mech. Res. Comm., Vol 4(5), 353-366, 1977.
- [6] Bazant, Z. P. and Wahab, A. B., Instability and Spacing of Cooling or Shrinkage Cracks, J. Engng. Mech. Div., ASCE, Vol 105, No EM5, 873-889, 1979.
- [7] Bazant, Z. P., Ohtsubo, H. and Aoh, K., Stability and Post-Critical Growth of a System of Cooling or Shrinkage Cracks, Int. J. Frac., Vol 15, 5, 443-456, 1979.
- [8] Bazant, Z. P., Instability of Parallel Thermal Cracks and its Consequences for Hot-Dry Rock Thermal Generation, Thermal Stresses in Severe Environments, Eds Hasselman, D. P. H. and Heller, R. A., Plenum Press, New York, 169-181, 1980.
- [9] Bazant, Z. P. and Cedolin, L., Stability of Structures - Elastic, Inelastic, Fracture, and Damage Theories, Oxford University Press, 801-817, 1991.
- [10] Underwood, J. H., Parker, A. P., Cote, P. J. and Sopok, S., Compressive Thermal Yielding Leading to Hydrogen Cracking in a Fired Cannon, Accepted for presentation at ASME Pressure Vessels and Piping Conference, San Diego, CA, 26-30 July 1998 and submitted to Trans ASME Journal of Pressure Vessel Technology.
- [11] Rooke, D. P., Baratta, F. I. and Cartwright, D. J., Simple Methods of Determining Stress Intensity Factors, Engng. Fracture Mech., 14, 2, 397-426, 1981.
- [12] Perl, M., Stress Intensity Factor Approximate Formulae for Uniform Crack Arrays in Pressurized or Autofrettaged Cylinders, Engng. Fracture Mech., 43, 5, 725-732, 1992.
- [13] Perl, M., Wu, K. H., Arone, R., Uniform Arrays of Unequal-Depth Cracks in Thick-Walled Cylindrical Pressure Vessels - Part I : Stress Intensity Factors Evaluation, Trans ASME, Journal of Pressure Vessel Technology, 112, 4, 340-345, 1990.
- [14] Parker, A. P., Some Comments on Work Relating to Stress Intensity in Arrays of Unequal-Depth Cracks, In preparation, 1998.

[15] Andrasic, C. P. and Parker, A. P., Spline Fit Weight Function Data for Cracked Thick Cylinders, Royal Military College of Science Technical Note MAT/36, Shrivenham, England, 1982.

[16] Andrasic, C. P., and Parker, A. P., Dimensionless Stress Intensity Factors for Cracked Thick Cylinders Under Polynomial Crack Face Loadings, Engng. Fracture Mech., 19, 1, 187-193, 1984.

[17] Nakasa, K., Takata, S., and Ichigi, H., An Analysis of Island-Delamination Type Cracking Pattern in the Brittle Film Coated on a Disk Under Axisymmetric Tension, Engng. Fracture Mech., 59, 2, 191-202, 1998.

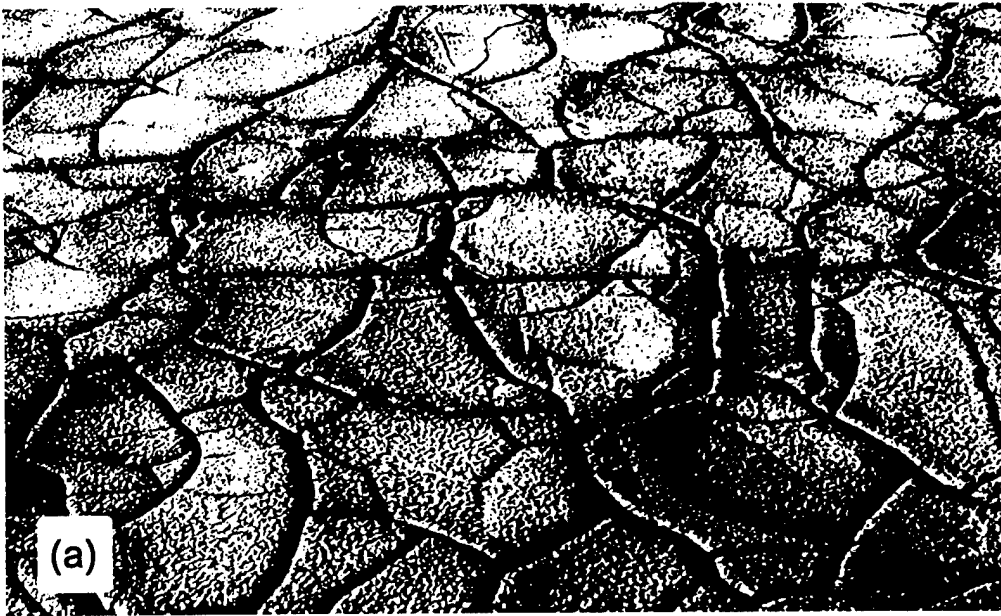


**Figure 1 : Surface Topographies. (a) Dried-out Mud Flats in Death Valley, typical plate size 250mm (b) Craze-Cracks (Heat-Checking) on Bore of a Gun Tube, typical plate size 0.6mm [3].**

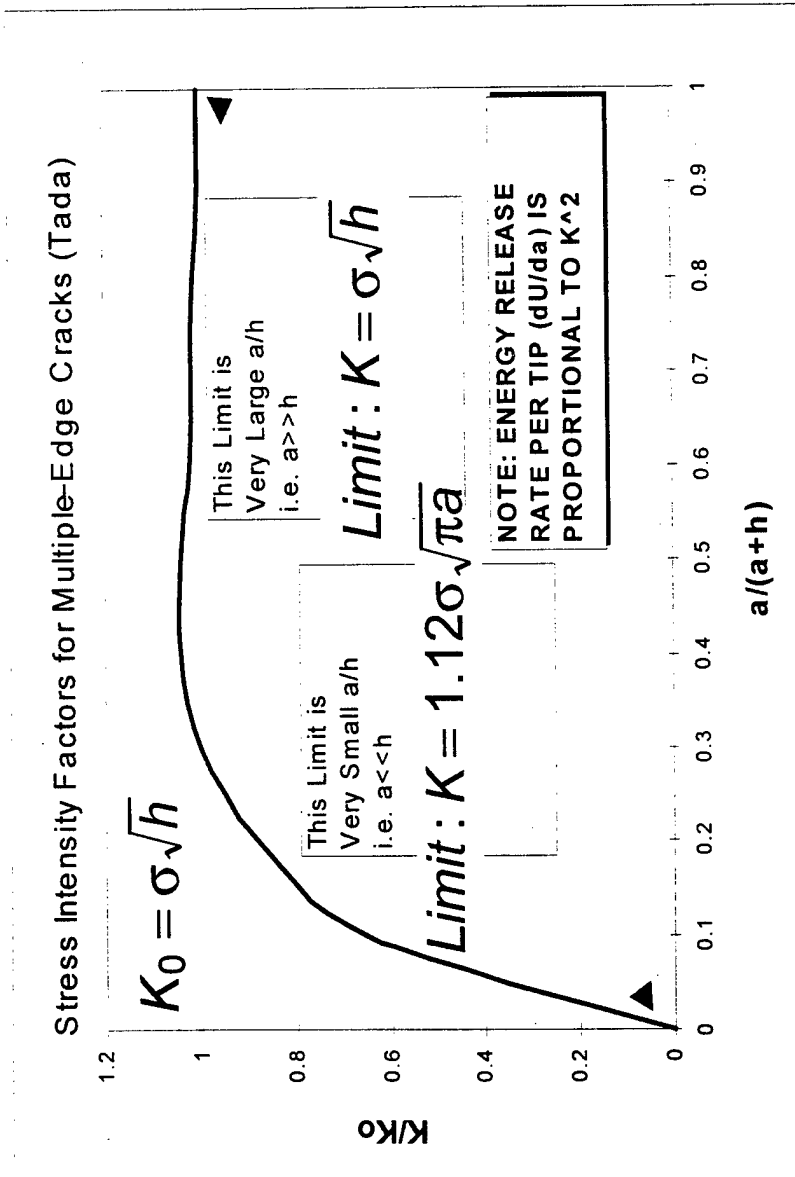
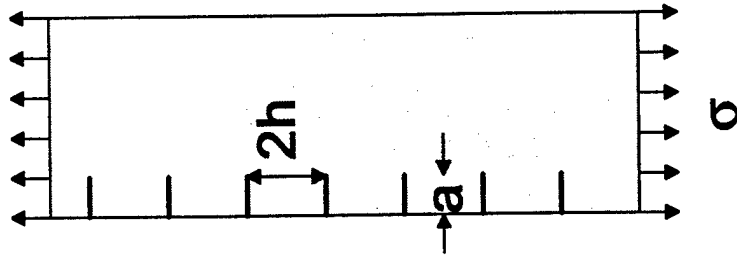
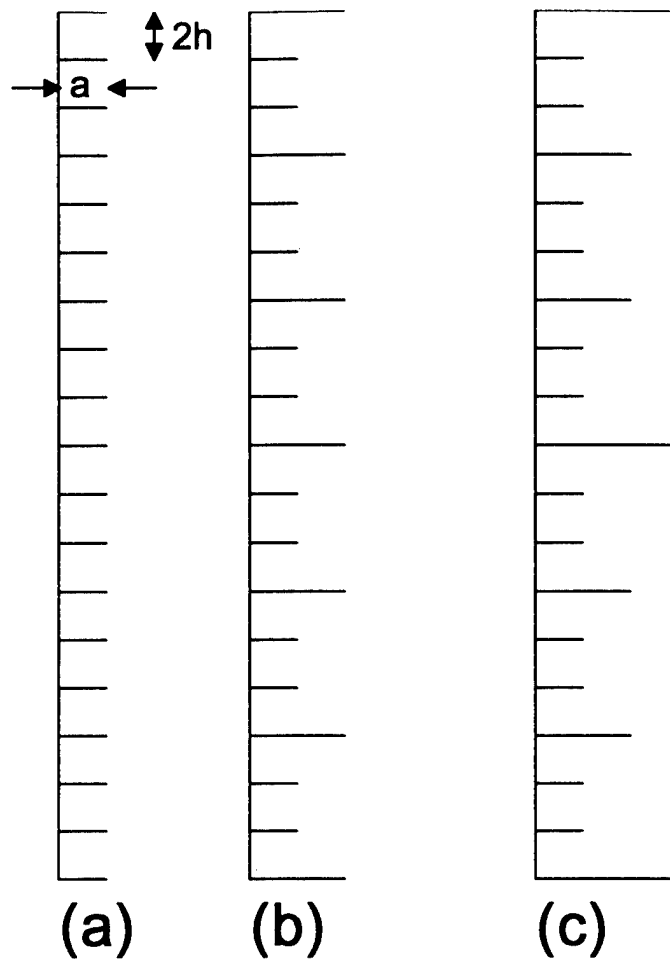


Figure 2 : Edge Cracks and Associated Stress Intensity Factors (after [4]).



**Figure 3 :**

- (a) Array of equal-length edge cracks**
- (b) Situation after first shedding of  $2/3$  of cracks**
- (c) Situation after second shedding of  $2/3$  of cracks**



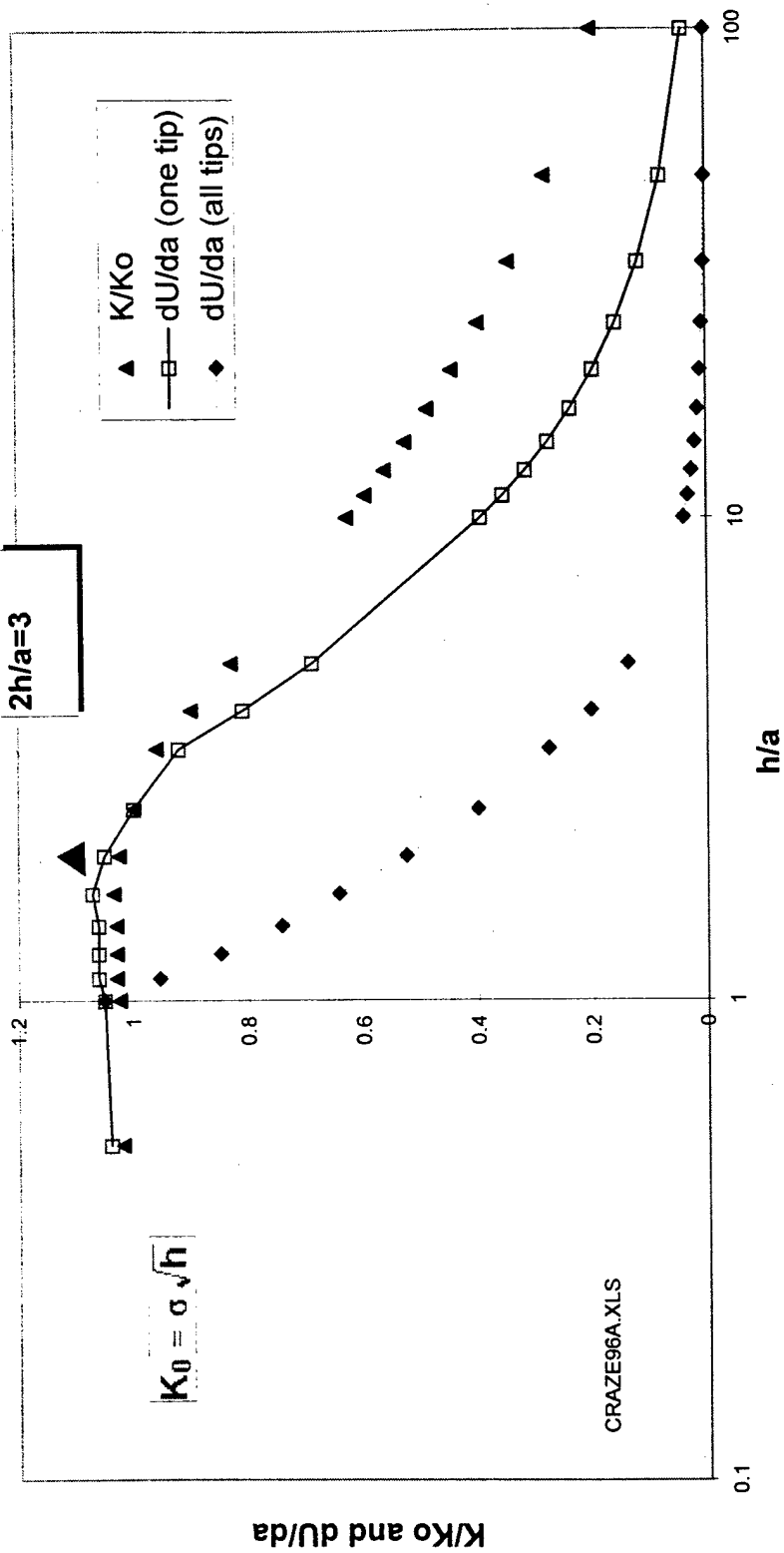


Figure 4 : Variation of Normalized Stress Intensity (Triangles) and of per tip (Squares) and Total Energy Release Rate (Diamonds) as a Function of h/a.  
Note : dU/da Scaled for Presentation on a Single Figure.

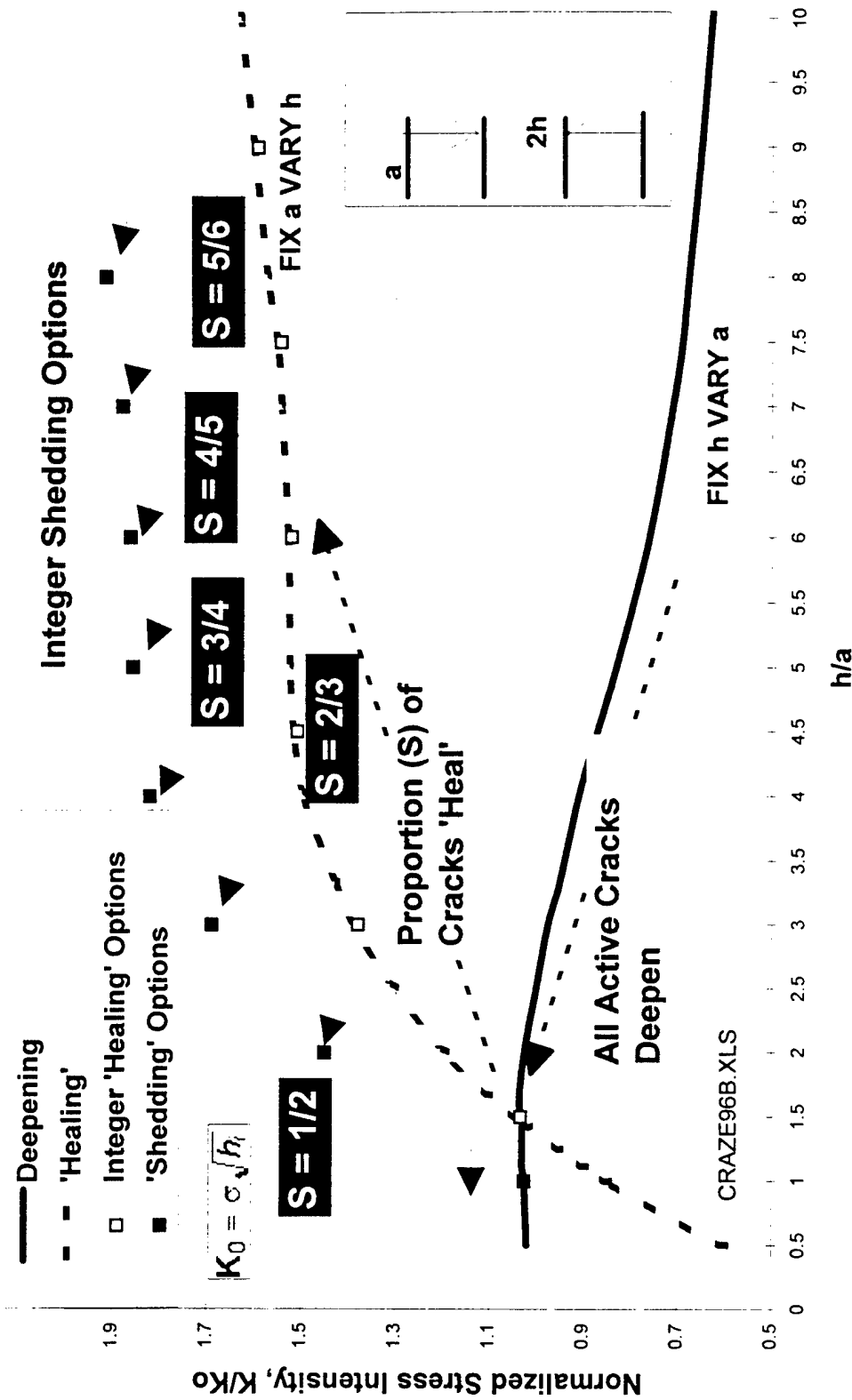
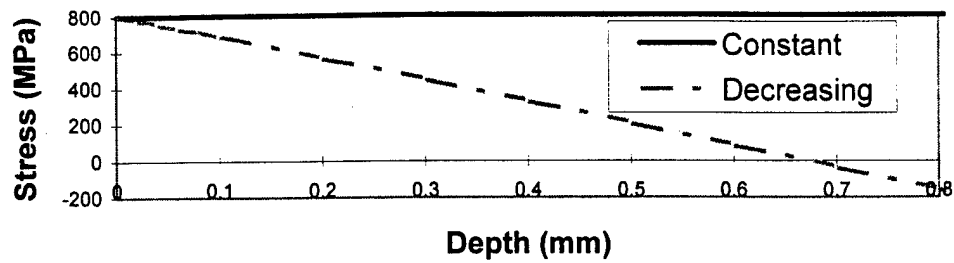
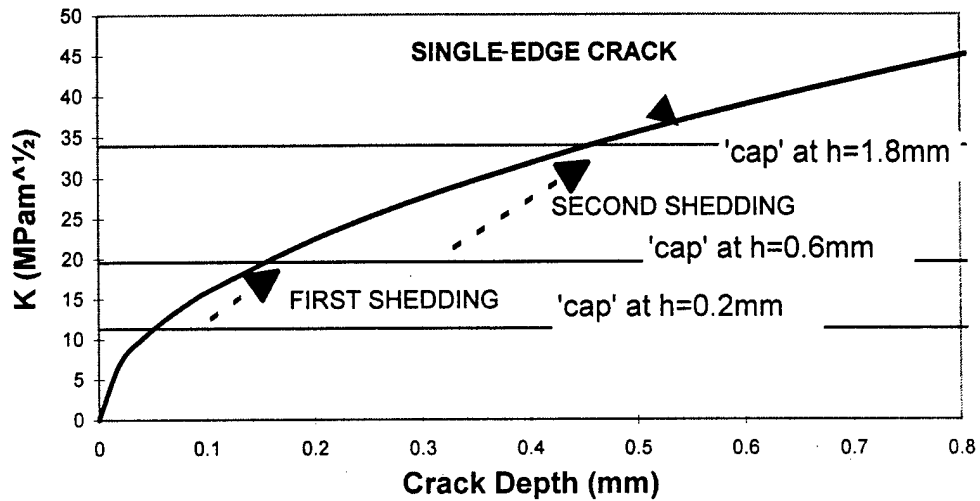


Figure 5 : Variation of Stress Intensity with  $h/a$ .  
 Lower curve,  $h$  fixed,  $a$  varying; upper curve,  $a$  fixed,  $h$  varying  
 Filled Squares - Situation After Further Crack Deepening.

(a) Assumed Stress Variation



(b) Variation of Stress Intensity (Constant Stress)



(c) Variation of Stress Intensity (Decreasing Stress)

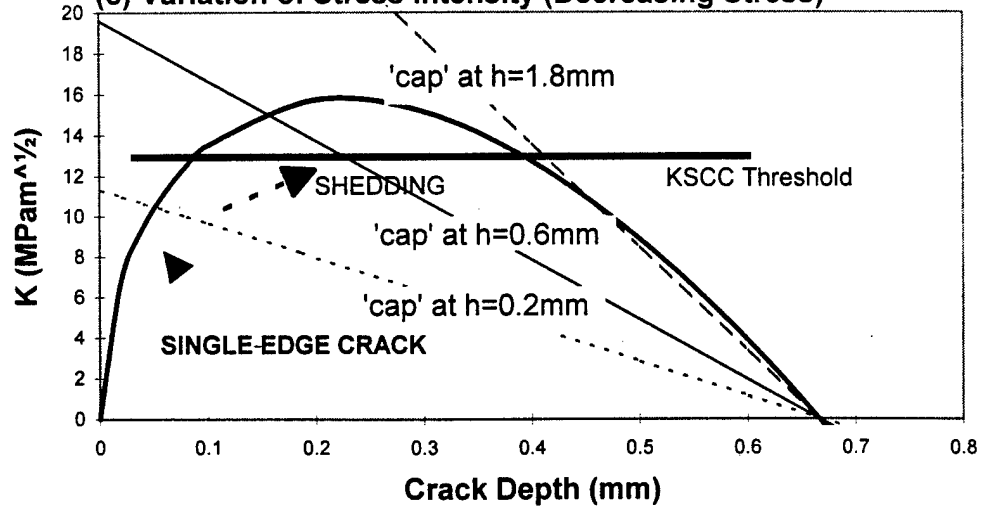


Figure 6 : (a) Stress Profiles (b) Stress Intensity (Constant Stress)  
(c) Stress Intensity (Linearly Decreasing Stress)

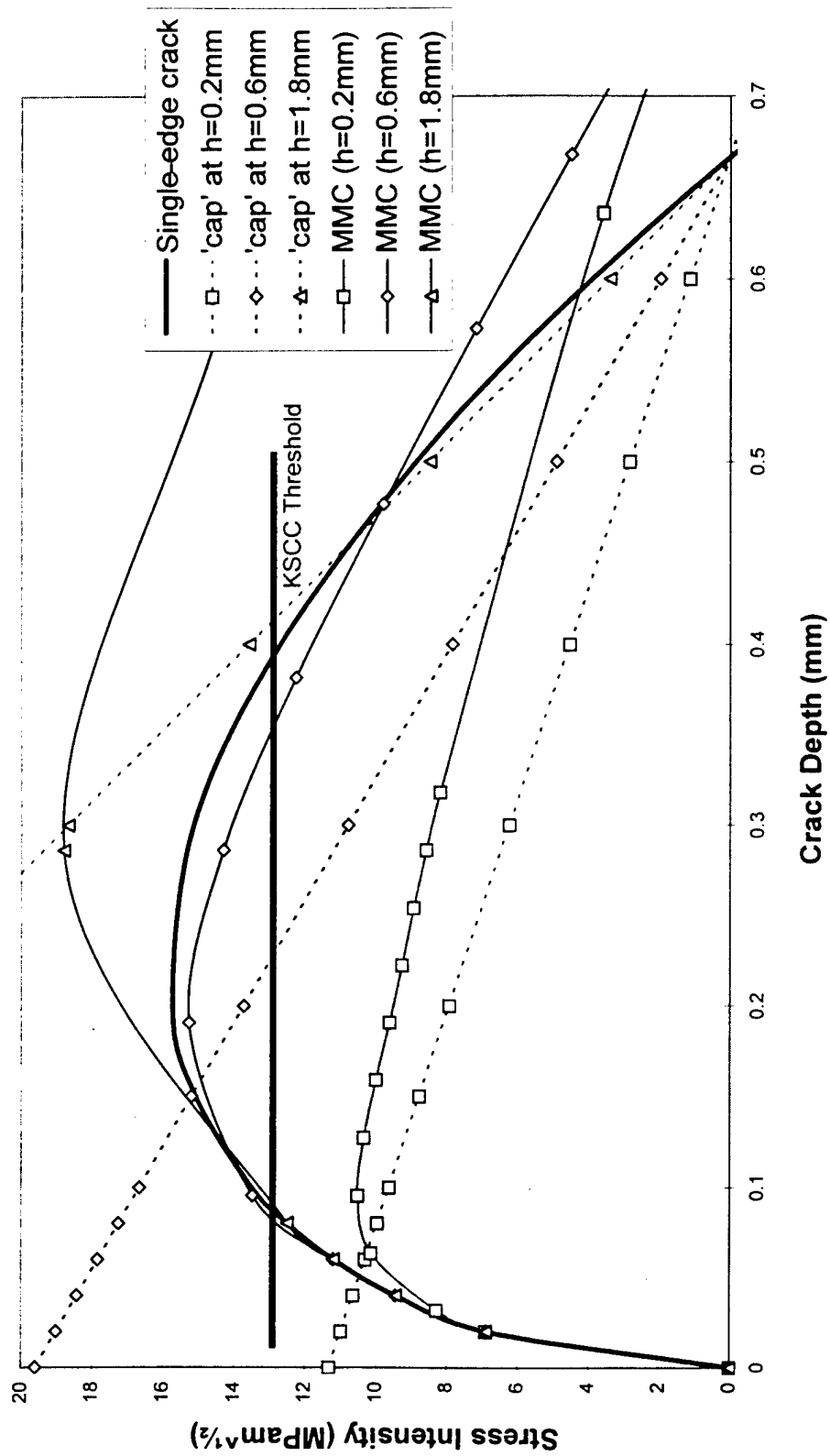


Figure 7 : Comparison of Approximations  
with Actual K Values (Decreasing Stress Profile)

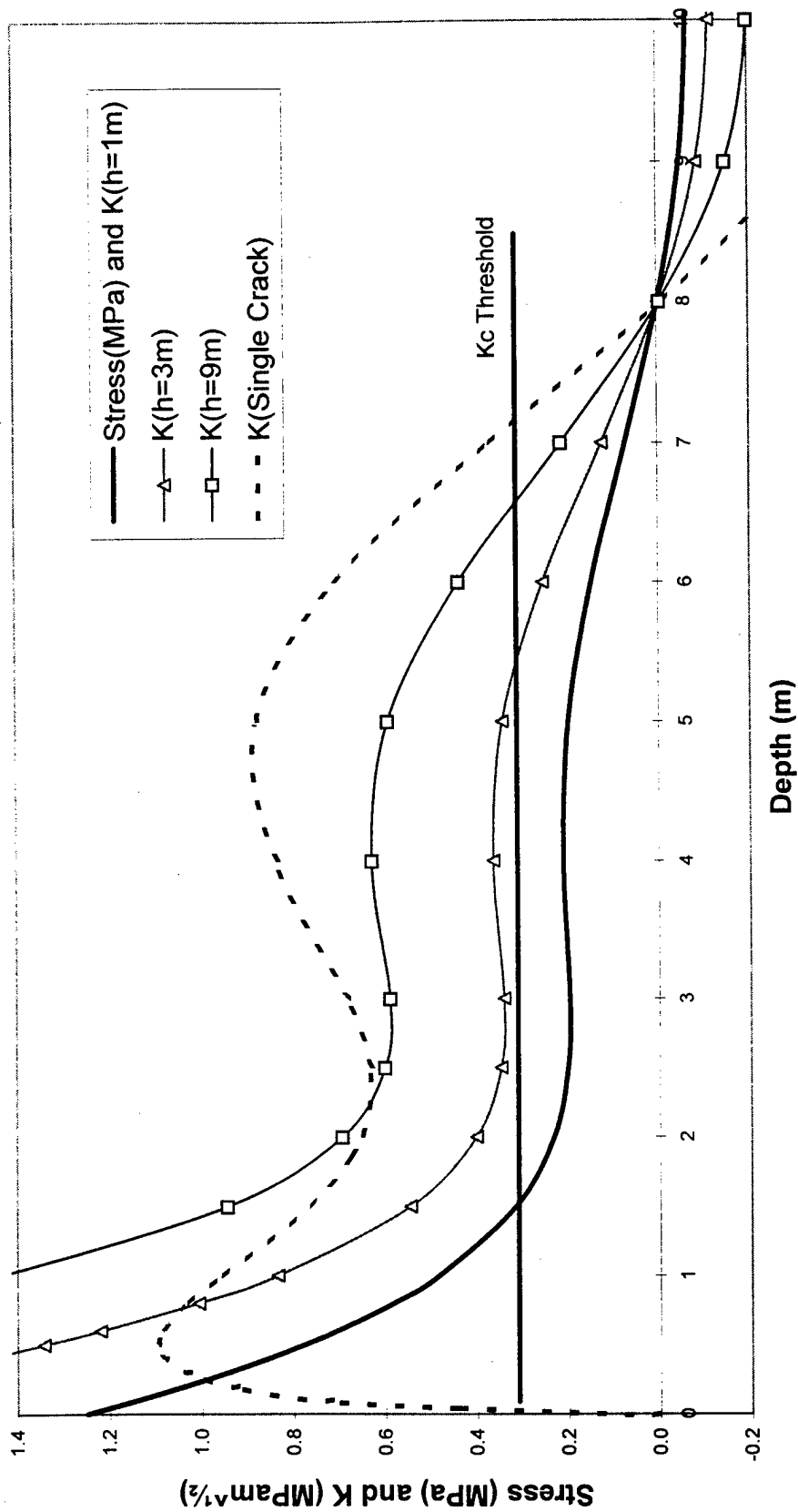


Figure 8 : Stress Distribution and Associated Approximate Stress Intensity Factors for Typical Arctic Permafrost Scenario in Early February.

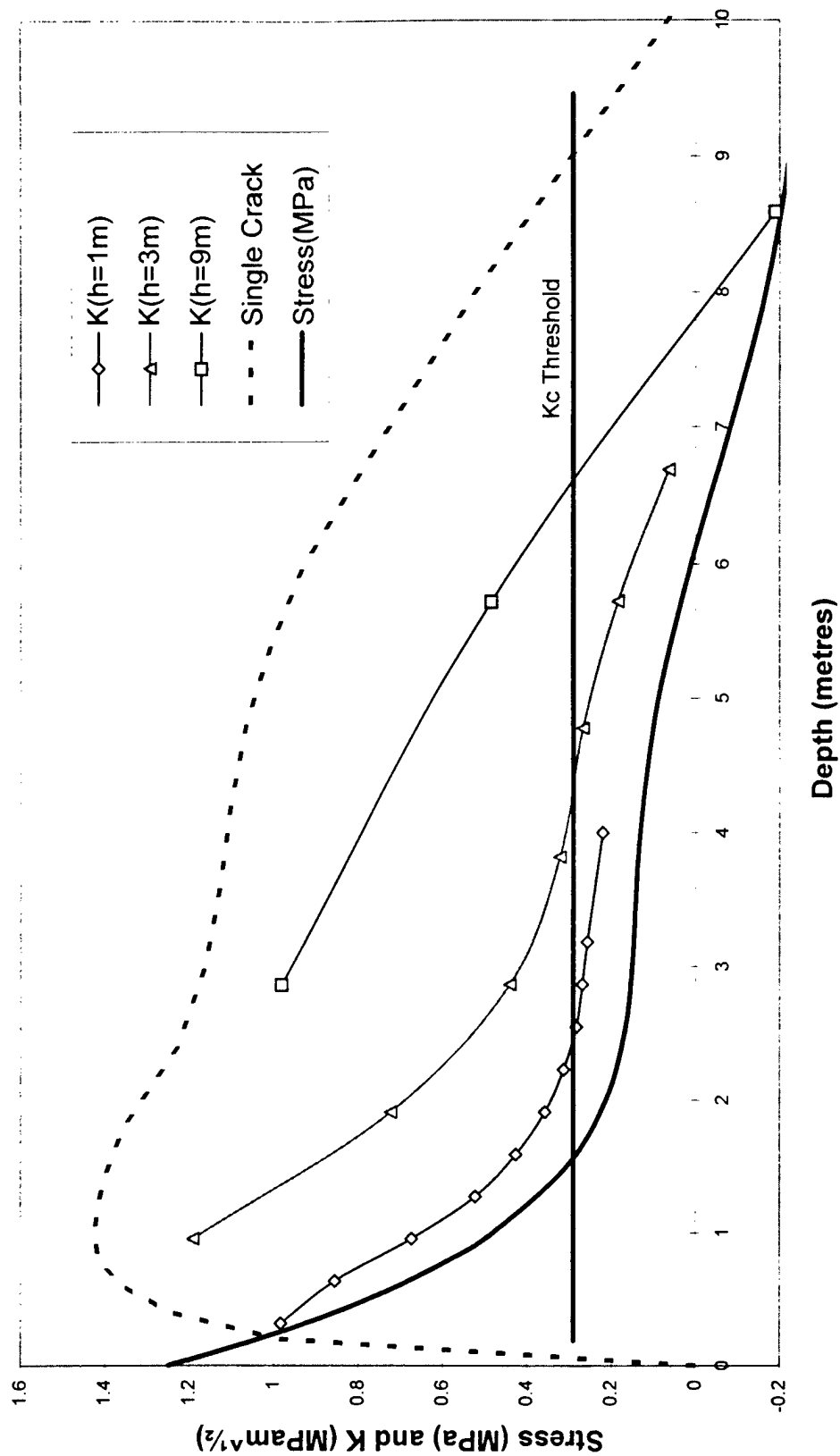


Figure 9 : Stress Distribution and Associated Accurate Stress Intensity Factors for Typical Arctic Permafrost Scenario in Early February. (MMC Solutions)



*Figure 10 : Micrograph of Edge-Cracking in a Gun Tube.  
Depth of large cracks 0.5mm (after [3])*

---

TECHNICAL REPORT INTERNAL DISTRIBUTION LIST

	<u>NO. OF COPIES</u>
CHIEF, DEVELOPMENT ENGINEERING DIVISION	
ATTN: AMSTA-AR-CCB-DA	1
-DB	1
-DC	1
-DD	1
-DE	1
CHIEF, ENGINEERING DIVISION	
ATTN: AMSTA-AR-CCB-E	1
-EA	1
-EB	1
-EC	1
CHIEF, TECHNOLOGY DIVISION	
ATTN: AMSTA-AR-CCB-T	2
-TA	1
-TB	1
-TC	1
TECHNICAL LIBRARY	
ATTN: AMSTA-AR-CCB-O	5
TECHNICAL PUBLICATIONS & EDITING SECTION	
ATTN: AMSTA-AR-CCB-O	3
OPERATIONS DIRECTORATE	
ATTN: SIOWV-ODP-P	1
DIRECTOR, PROCUREMENT & CONTRACTING DIRECTORATE	
ATTN: SIOWV-PP	1
DIRECTOR, PRODUCT ASSURANCE & TEST DIRECTORATE	
ATTN: SIOWV-QA	1

NOTE: PLEASE NOTIFY DIRECTOR, BENÉT LABORATORIES, ATTN: AMSTA-AR-CCB-O OF ADDRESS CHANGES.

---



---

TECHNICAL REPORT EXTERNAL DISTRIBUTION LIST

	<u>NO. OF COPIES</u>		<u>NO. OF COPIES</u>
ASST SEC OF THE ARMY RESEARCH AND DEVELOPMENT ATTN: DEPT FOR SCI AND TECH THE PENTAGON WASHINGTON, D.C. 20310-0103	1	COMMANDER ROCK ISLAND ARSENAL ATTN: SMCRI-SEM ROCK ISLAND, IL 61299-5001	1
DEFENSE TECHNICAL INFO CENTER ATTN: DTIC-OC (ACQUISITIONS) 8725 JOHN J. KINGMAN ROAD STE 0944 FT. BELVOIR, VA 22060-6218	2	COMMANDER U.S. ARMY TANK-AUTMV R&D COMMAND ATTN: AMSTA-DDL (TECH LIBRARY) WARREN, MI 48397-5000	1
COMMANDER U.S. ARMY ARDEC ATTN: AMSTA-AR-AEE, BLDG. 3022	1	COMMANDER U.S. MILITARY ACADEMY ATTN: DEPARTMENT OF MECHANICS WEST POINT, NY 10966-1792	1
AMSTA-AR-AES, BLDG. 321	1	U.S. ARMY MISSILE COMMAND	
AMSTA-AR-AET-O, BLDG. 183	1	REDSTONE SCIENTIFIC INFO CENTER	2
AMSTA-AR-FSA, BLDG. 354	1	ATTN: AMSMI-RD-CS-R/DOCUMENTS	
AMSTA-AR-FSM-E	1	BLDG. 4484	
AMSTA-AR-FSS-D, BLDG. 94	1	REDSTONE ARSENAL, AL 35898-5241	
AMSTA-AR-IMC, BLDG. 59	2		
PICATINNY ARSENAL, NJ 07806-5000		COMMANDER U.S. ARMY FOREIGN SCI & TECH CENTER ATTN: DRXST-SD 220 7TH STREET, N.E. CHARLOTTESVILLE, VA 22901	1
DIRECTOR U.S. ARMY RESEARCH LABORATORY ATTN: AMSRL-DD-T, BLDG. 305 ABERDEEN PROVING GROUND, MD 21005-5066	1	COMMANDER U.S. ARMY LABCOM, ISA ATTN: SLCIS-IM-TL 2800 POWER MILL ROAD ADELPHI, MD 20783-1145	1
DIRECTOR U.S. ARMY RESEARCH LABORATORY ATTN: AMSRL-WT-PD (DR. B. BURNS) ABERDEEN PROVING GROUND, MD 21005-5066	1		

---

NOTE: PLEASE NOTIFY COMMANDER, ARMAMENT RESEARCH, DEVELOPMENT, AND ENGINEERING CENTER,  
BENÉT LABORATORIES, CCAC, U.S. ARMY TANK-AUTOMOTIVE AND ARMAMENTS COMMAND,  
AMSTA-AR-CCB-O, WATERVLIET, NY 12189-4050 OF ADDRESS CHANGES.

---

TECHNICAL REPORT EXTERNAL DISTRIBUTION LIST (CONT'D)

	<u>NO. OF COPIES</u>		<u>NO. OF COPIES</u>
COMMANDER U.S. ARMY RESEARCH OFFICE ATTN: CHIEF, IPO P.O. BOX 12211 RESEARCH TRIANGLE PARK, NC 27709-2211	1	WRIGHT LABORATORY ARMAMENT DIRECTORATE ATTN: WL/MNM EGLIN AFB, FL 32542-6810	1
DIRECTOR U.S. NAVAL RESEARCH LABORATORY ATTN: MATERIALS SCI & TECH DIV WASHINGTON, D.C. 20375	1	WRIGHT LABORATORY ARMAMENT DIRECTORATE ATTN: WL/MNMF EGLIN AFB, FL 32542-6810	1

NOTE: PLEASE NOTIFY COMMANDER, ARMAMENT RESEARCH, DEVELOPMENT, AND ENGINEERING CENTER,  
BENÉT LABORATORIES, CCAC, U.S. ARMY TANK-AUTOMOTIVE AND ARMAMENTS COMMAND,  
AMSTA-AR-CCB-O, WATERVLIET, NY 12189-4050 OF ADDRESS CHANGES.

---